CHEMISTRY OF MATERIALS
Cite This: Chem. Mater. 2018, 30, 4864−4873
Article
pubs.acs.org/cm

Effect of Acceptor Unit Length and Planarity on the Optoelectronic Properties of Isoindigo−Thiophene Donor−Acceptor Polymers

Nicholas M. Randell,[†] Chase L. Radford,[†] Jinli Yang,[†] Jesse Quinn,[‡] Dongliang Hou,[‡] Yuning Li,[‡] and Timothy L. Kelly*[,†]

[†]Department of Chemistry, University of Saskatchewan, 110 Science Place, Saskatoon, Saskatchewan S7N 5C9, Canada
[‡]Department of Chemical Engineering and Waterloo Institute for Nanotechnology (WIN), University of Waterloo, 200 University Avenue West, Waterloo, Ontario N2L 3G1, Canada

Supporting Information

ABSTRACT: Conjugated polymers with a donor−acceptor (DA) structural motif have found extensive use in a wide variety of optoelectronic devices; however, despite their ubiquity in the literature, the vast majority of these materials are simple alternating copolymers—one electron donor alternates with one electron acceptor in the polymer backbone. As a result, the impact of composition (e.g., donor/acceptor ratio) and structure (e.g., alternating, block, or random) on the optoelectronic properties of these copolymers remains poorly understood. In this work, the number of acceptor units in alternating DA copolymers is systematically increased. Two dimers of the common electron acceptor isoindigo are synthesized, one with free rotation between the subunits and one with enforced coplanarity. The two dimers are then used to synthesize donor−acceptor−acceptor (DAA) copolymers with either thiophene or terthiophene comonomers. These DAA polymers feature two electron acceptors in their repeat unit, and their optoelectronic properties are compared to those of the analogous DA polymers. It is shown that increasing the number of acceptor units causes a decrease in the LUMO energy of the resulting polymer; this effect is enhanced by enforcing coplanarity between acceptor units via ring fusion. All six polymers were tested in both organic photovoltaics (OPVs) and organic thin film transistors (OTFTs). While the DA polymers performed better in OPVs, the DAA polymers displayed more balanced charge carrier mobilities in OTFTs.

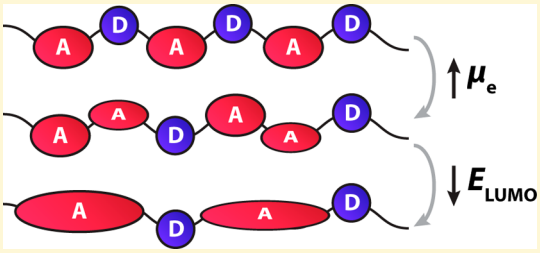

INTRODUCTION

Organic electronic devices, such as organic photovoltaics (OPVs) and organic thin film transistors (OTFTs), have made great strides in key figures of merit over the past two decades because of advances in the design and synthesis of donor−acceptor (DA) copolymers.[1−3] These materials are composed of alternating electron-rich (donor) and electron-poor (acceptor) units.[4] This results in the partial isolation of the frontier molecular orbitals; the donor makes the greatest contribution to the highest occupied molecular orbital (HOMO), while the lowest unoccupied molecular orbital (LUMO) has more acceptor character. This results in low-band gap materials that can absorb in the near-infrared region.[5] Common donor units include oligothiophenes, thienothiophenes, and benzodithiophene; typical acceptor units incorporate either electron-withdrawing functional groups (e.g., amides, imides, and cyano) or electronegative halogen atoms.[6−11]

Conventional DA polymers have a repeat unit consisting of a simple donor−acceptor pair. Recently, several research groups have investigated the effects of increasing the number of donor units in DA copolymers, often by varying the number of thiophenes in an oligothiophene donor. Zhou et al. varied the number of thiophene donors in a series of DA polymers with two different acceptor units, thieno[3,4-*c*]pyrrole-4,6-dione (TPD) and bithiopheneimide (BTI).[12] They showed that the polymers' HOMO energy increased with the length of the thiophene block. Additionally, the conjugation length of the polymers also increased with the number of thiophene units, reaching its maximum with a terthiophene donor. Both the TPD-based and BTI-based polymers were used in OPVs, and when compared, the power conversion efficiencies (PCEs) were found to be greater for the terthiophene-containing polymers. Similar studies have also been performed using isoindigo [**iI** (Chart 1)] as the acceptor unit.[13,14] Ma et al. synthesized isoindigo−oligothiophene polymers containing one, three, five, and six thiophenes in the repeat unit.[13] The LUMO level was identical for all four polymers, while the HOMO levels increased with the number of thiophenes. The terthiophene copolymer had the narrowest optical band gap ($E_{g,opt}$), and it was found that longer donor units did not further red-shift the absorbance profiles; the best OPV efficiency was also achieved with the isoindigo−terthiophene polymer. Transmission electron microscopy and grazing-incidence wide-angle X-ray scattering (GIWAXS) measurements showed that donor units larger than terthiophene led to aggregation in the active layer, resulting in a loss of PCE.

Received: June 15, 2018
Revised: June 19, 2018
Published: June 20, 2018

Chem. Mater. 2018.30:4864-4873.
Downloaded from pubs.acs.org by UNIV OF SUNDERLAND on 10/05/18. For personal use only.

© 2018 American Chemical Society

DOI: 10.1021/acs.chemmater.8b02535
Chem. Mater. 2018, 30, 4864−4873

Chart 1. Isoindigo (iI), Diisoindigo (di-iI), and Bisisoindigo (bis-iI)

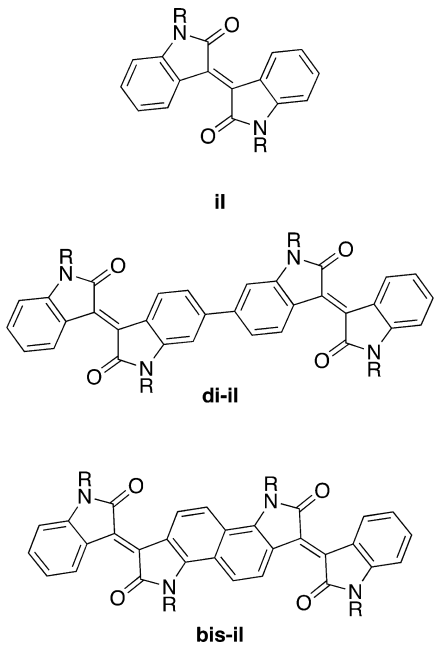

Following this, Reynolds and co-workers investigated the OPV performance of isoindigo−thiophene (**iI-T**) and isoindigo−terthiophene (**iI-3T**) copolymers.[15−17] Despite the similar optoelectronic properties of the two polymers, OPVs fabricated with **iI-3T** were more than twice as efficient as those made using **iI-T**. They discovered that **iI-3T**:$PC_{71}BM$ films had relative permittivities higher than those of **iI-T**:$PC_{71}BM$ blends; this implied better electronic coupling between **iI-3T** and $PC_{71}BM$. The improved coupling promoted faster exciton dissociation, leading to the increase in PCE.[16]

This work clearly shows that the number of donor units in a DA copolymer can significantly impact optoelectronic properties, film morphology, and device performance. Yet despite the numerous studies of oligothiophene donors, there is a paucity of work examining copolymers with multiple acceptor subunits (presumably because the synthesis of electron-deficient oligomers is more complex than the synthesis of oligothiophenes). One acceptor that could be useful in such a study is isoindigo. Isoindigo was first used as the electron acceptor in DA systems by Mei et al.[18] and has since become a common acceptor unit in many organic semiconductors.[18−27] Modified isoindigo structures, such as thienoisoindigo and other ring-fused derivatives, have also recently been explored.[28−35] Thienoisoindigo and its derivatives are readily brominated, making dimers synthetically accessible.[28,29,36] James et al. used this approach to synthesize a thieno−benzoisoindigo dimer,

Chart 2. Structures of the DA Copolymers (iI-T, iI-3T) and the DAA Copolymers (di-iI-T, di-iI-3T; bis-iI-T, bis-iI-3T) in This Study

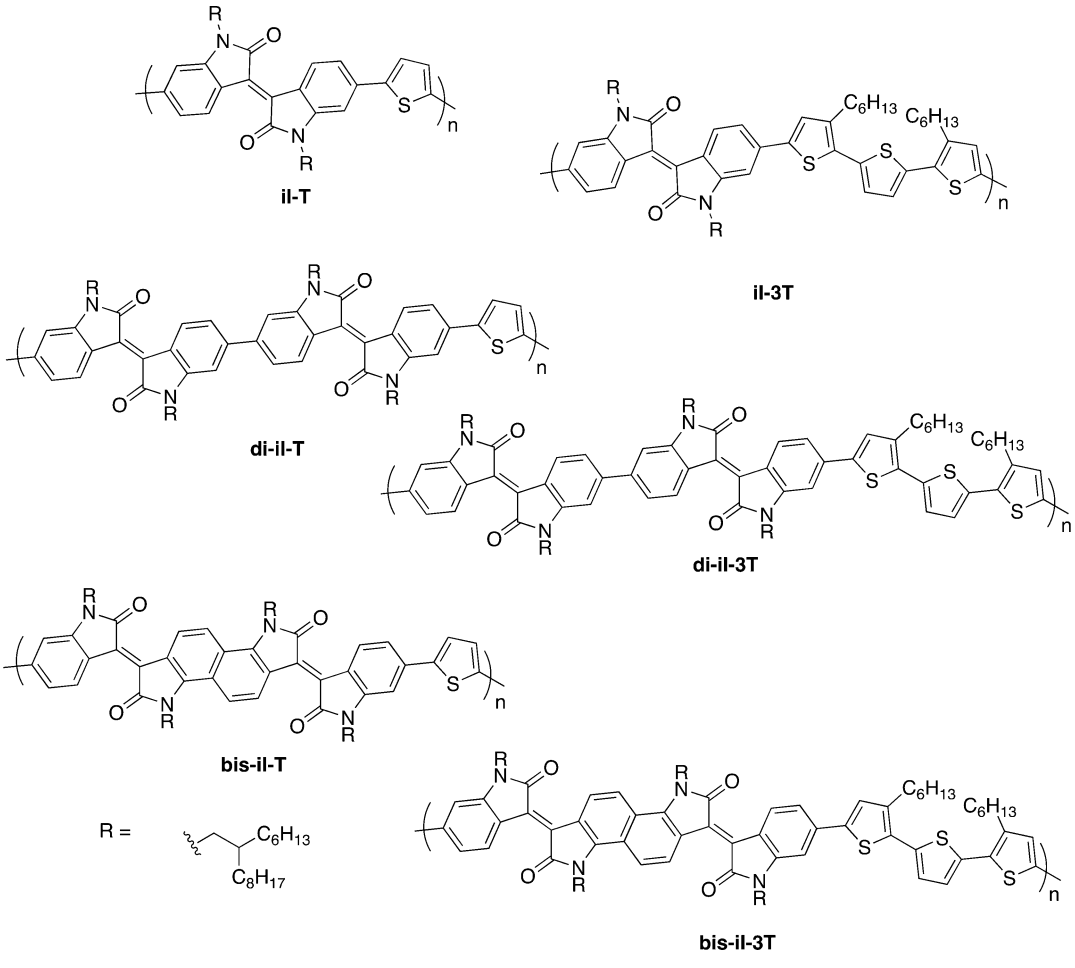

DOI: 10.1021/acs.chemmater.8b02535
Chem. Mater. 2018, 30, 4864−4873

Scheme 1. Synthesis of Dibromodiisoindigo (Br_2-di-iI)

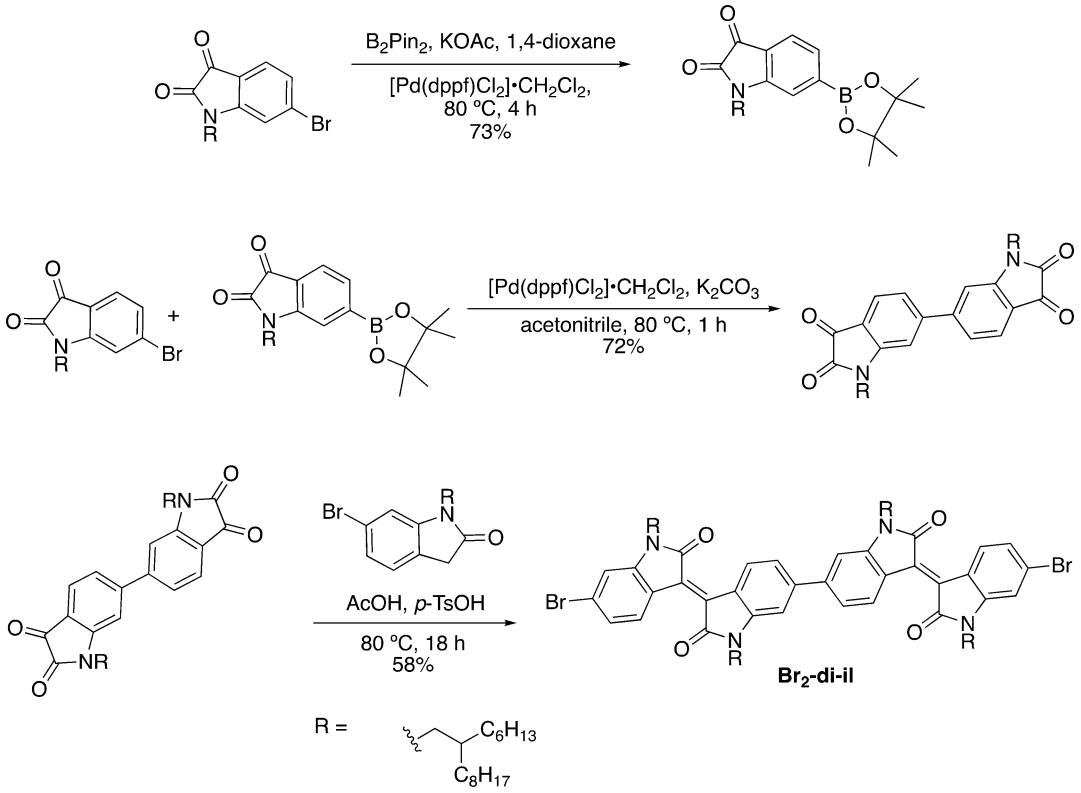

which was subsequently incorporated into a polymer.[37] These DAA polymers featured a repeat structure of one donor unit and two acceptor units. They were used to fabricate OTFTs, revealing a high hole mobility (μ_h = 1.1 $cm^2\ V^{-1}\ s^{-1}$) and ambipolar charge transport behavior ($\mu_e = 6.6 \times 10^{-3}\ cm^2\ V^{-1}\ s^{-1}$).[37] In 2016, we reported a small molecule DA system based on bisisoindigo (**bis-iI**), an isoindigo dimer in which the two halves are ring-fused across positions 6 and 7 (Chart 1);[38] the coplanarity substantially reduced the $E_{g,opt}$ relative to that of isoindigo. Shortly thereafter, Jiang et al. incorporated **bis-iI** into a series of DAA polymers, which were shown to have balanced charge carrier mobilities (μ_h = 1.79 $cm^2\ V^{-1}\ s^{-1}$, and μ_e = 0.087 $cm^2\ V^{-1}\ s^{-1}$).[39] Very recently, Xu et al. produced a series of DAA polymers in which the two isoindigo acceptor units are bridged by a vinyl spacer.[40] The polymer containing fluoroisoindigo acceptors and a bithiophene donor unit exhibited excellent ambipolar charge transport characteristics (μ_h = 1.03 $cm^2\ V^{-1}\ s^{-1}$, and μ_e = 1.82 $cm^2\ V^{-1}\ s^{-1}$), owing to its highly planar nature.

Herein, we describe the synthesis of an isoindigo dimer, diisoindigo [**di-iI** (Chart 1)]; in this case, two isoindigo subunits are joined by a single bond at position 6. Using **di-iI** and **bis-iI**, we have synthesized four DAA copolymers featuring either a thiophene or terthiophene donor unit; for comparison, we also synthesized the analogous **iI** polymers (Chart 2). Via comparison of the **iI** and **di-iI** polymers, the effect of adding a second acceptor to the repeat unit of a DA copolymer was studied. Additionally, comparing the **di-iI** and **bis-iI** polymers allowed us to evaluate the impact of planarizing the two acceptor units. We show that altering the number of acceptor units in a DA copolymer is a viable strategy for fine-tuning both the LUMO energy and the charge transport properties of the material; the effect is magnified when the acceptor units are forced to adopt a more coplanar geometry.

RESULTS AND DISCUSSION

The synthesis of both **bis-iI** and **di-iI** involves first synthesizing the appropriate isatin dimer (either ring-fused or connected at positions 6 and 6′), followed by two concurrent crossed-aldol condensations with 6-bromo-2-oxindole to form the desired dihalogenated isoindigo dimer; the synthesis of dibrominated monomer **Br_2-di-iI** is shown in Scheme 1. First, the 6-bromoisatin is alkylated, and then a Miayura coupling is used to generate the boronic ester-functionalized isatin. The 6-isatinboronate ester and an equivalent of the 6-bromoisatin are combined in a Suzuki coupling to form the 6,6′-diisatin dimer in moderate yield. Finally, the dihalogenated **Br_2-di-iI** dimer (Scheme 1) is synthesized by a double crossed-aldol reaction.

In our previous report on **bis-iI**, the central ring-fused isatin dimer was first synthesized by the Martinet isatin synthesis and subsequently alkylated using 2-ethylhexyl iodide, to produce a soluble product.[38] However, in this work, longer 2-hexyldecyl alkyl groups were required to solubilize the DAA polymers. It was found that the size of these bulkier alkyl chains prevented the effective alkylation of the lactam nitrogens; therefore, we employed a new synthetic method to produce dibrominated monomer **Br_2-bis-iI** (Scheme S1). In this synthesis, 1,5-diaminonaphthalene is first alkylated before being subjected to the Martinet isatin synthesis and subsequent aldol condensations, producing **Br_2-bis-iI**.[39]

All six polymers (Chart 2) were then synthesized by palladium-catalyzed Stille polymerizations. **iI-T** and **iI-3T** were synthesized according to procedures reported by Stalder et al.[15] Likewise, **di-iI-T** and **bis-iI-T** were synthesized by polymerization of the extended isoindigo monomer (**Br_2-di-**

DOI: 10.1021/acs.chemmater.8b02535
Chem. Mater. 2018, 30, 4864−4873

Table 1. Molecular Weights, Dispersities, and Optoelectronic Properties of All Polymers

polymer	M_w (kDa)	M_n (kDa)	$Đ$	$E_{g,elec}$ [a] (eV)	$E_{g,opt}$ (eV)	μ_h [b] ($cm^2\ V^{-1}\ s^{-1}$)	μ_e [b] ($cm^2\ V^{-1}\ s^{-1}$)
iI-T	93	37	2.5	1.90	1.61	$(9 \pm 1) \times 10^{-4}$	$(5.1 \pm 0.9) \times 10^{-4}$
iI-3T	80	27	3.0	1.72	1.57	$(4.1 \pm 0.4) \times 10^{-3}$	n/a
di-iI-T	55	17	3.2	1.88	1.60	$(1.6 \pm 0.2) \times 10^{-3}$	$(1.3 \pm 0.5) \times 10^{-3}$
di-iI-3T	51	21	2.4	1.73	1.54	$(9 \pm 4) \times 10^{-4}$	$(2.3 \pm 0.3) \times 10^{-3}$
bis-iI-T	52	20	2.6	1.64	1.30	$(1.5 \pm 0.1) \times 10^{-3}$	$(1.7 \pm 0.6) \times 10^{-3}$
bis-iI-3T	69	25	2.8	1.62	1.31	$(2.6 \pm 0.3) \times 10^{-3}$	$(6 \pm 1) \times 10^{-4}$

[a] $E_{g,elec} = E_{LUMO} - E_{HOMO}$. [b] μ_h and μ_e values determined from OTFT measurements of an average of five devices.

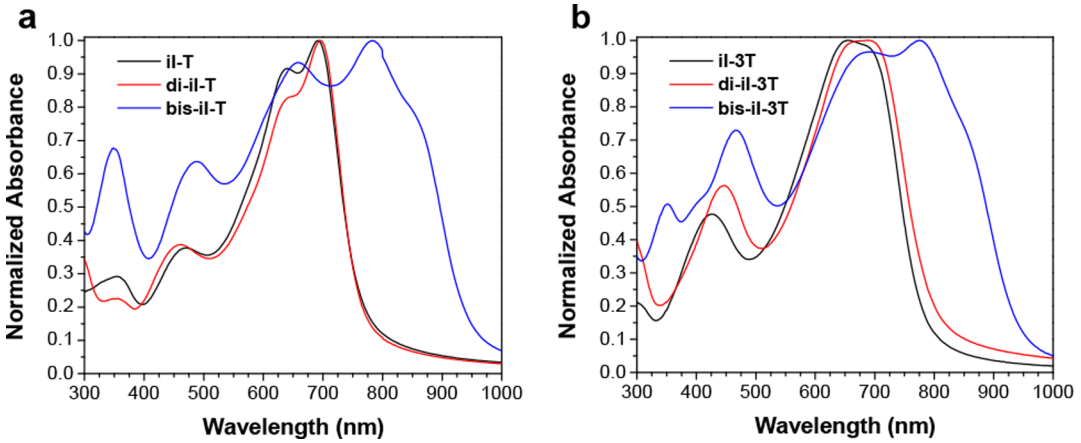

Figure 1. Thin film UV−vis spectra of (a) **iI-T**, **di-iI-T**, and **bis-iI-T** and (b) **iI-3T**, **di-iI-3T**, and **bis-iI-3T**.

iI and **Br_2-bis-iI**) with 2,5-bis(trimethylstannyl)thiophene. Because of the difficulty purifying the bis(trimethylstannyl)-terthiophene comonomer used by Stalder et al.,[15] both **di-iI-3T** and **bis-iI-3T** were synthesized by methods analogous to those used by Wang et al.[22] to synthesize **iI-3T** (Schemes S2 and S3). First, the extended isoindigo (**Br_2-di-iI** or **Br_2-bis-iI**) was coupled to 2 equiv of 2-trimethylstannyl-4-hexylthiophene; the product was brominated twice, and a Stille polycondensation with 2,5′-bis(trimethylstannyl)thiophene was used to produce polymers **di-iI-3T** and **bis-iI-3T** (Schemes S2 and S3). All six polymers had weight-average molecular weights (M_w) between 51 and 93 kDa and number-average molecular weights (M_n) between 17 and 37 kDa (Table 1), as determined by size exclusion chromatography (SEC). The M_n values of the DAA polymers were all lower than those of their DA counterparts, possibly because of the lower overall solubility of these polymers. The molecular weights of **iI-T** and **iI-3T**, while reasonable, were slightly lower than those reported by Stalder et al.[17] After purification by Soxhlet extraction, the dispersity ($Đ$) of all of the polymers was between 2.4 and 3.2. This is in line with the expectations for a step-growth polycondensation ($Đ \geq 2$) and perhaps indicates that the Soxhlet fractionation process removed only monomers and very short oligomers and had little impact on the overall dispersity.

On the basis of the work of Zhou et al.[12] and Ma et al.[13] (where increasing the number of thiophene donors was found to increase the HOMO energy), here we expected that increasing the number of acceptors in the polymer repeat unit would lower the LUMO energy of the resulting polymers; the lower LUMO energy should therefore reduce $E_{g,opt}$ for the **di-iI-** and **bis-iI**-based polymers relative to those of their **iI** counterparts. However, the ultraviolet−visible (UV−vis) spectra of polymer thin films (Figure 1) show that the **iI** and **di-iI** polymers have similar $E_{g,opt}$ values, with only the **bis-iI** polymers displaying the expected red-shift in absorbance (Table 1). The narrow band gap of the **bis-iI** polymers is due to the coplanar nature of the two isoindigo units in this dimer (Figure 2). When there is free rotation between adjacent

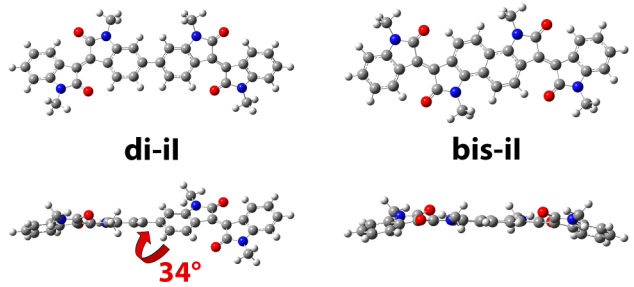

Figure 2. Optimized geometries of **di-iI** and **bis-iI**, calculated at the B3LYP/6-31G(d,p) level of theory.

acceptor units, as in the **di-iI**-containing polymers, steric repulsion forces them to adopt a twisted geometry. The large dihedral angle between adjacent isoindigo units limits the degree of conjugation, diminishing the effect of having two acceptors in the polymer repeat unit. This is especially clear when comparing the spectra of **iI-T** and **di-iI-T**; the $E_{g,opt}$ of **di-iI-T** is red-shifted by only 5 nm relative to that of **iI-T**. While the red-shift is slightly more pronounced between **iI-3T** and **di-iI-3T**, the $E_{g,opt}$ of **di-iI-3T** is still much larger than that of the more coplanar **bis-iI-3T**.

Density functional theory (DFT) calculations [B3LYP/6-31G(d,p)] were performed on **di-iI** and **bis-iI** to determine their optimized geometries, as well as the isosurfaces and eigenvalues of the frontier molecular orbitals. The optimized geometry of **di-iI** has the expected large dihedral angle (34°)

DOI: 10.1021/acs.chemmater.8b02535
Chem. Mater. 2018, 30, 4864−4873

between the isoindigo groups (Figure 2). This supports the theory that backbone twisting is responsible for the relatively small change in the $E_{g,opt}$ of the **di-iI** polymers as compared to that of their **iI** analogues; the enforced planarity in **bis-iI** results in a flatter structure (Figure 2). Similar calculations were performed on oligomeric models of all six polymers. In all three thiophene copolymers, the frontier molecular orbitals are delocalized across the entire repeat unit (Figures S1−S3). However, the effect of the increasing acceptor length is noticeable in the frontier orbitals of the terthiophene copolymers (Figures S4−S6). In the LUMO of **iI-3T**, there is still significant electron density on the central terthiophene; in the LUMOs of **di-iI-3T** and **bis-iI-3T**, there is almost no electron density remaining on the terthiophene unit, as the increased acceptor strength of the **di-iI** and **bis-iI** units results in less orbital mixing.

Cyclic and differential pulse voltammetry were used to study the electrochemical behavior of the polymers and to estimate the energies of their frontier molecular orbitals. The oxidation of the polymers is largely governed by the identity of the donor unit (Figures S7−S9). All six polymers exhibit irreversible oxidation; this process happens at a lower potential versus Fc/Fc^+ for the polymers containing terthiophene than those containing the weaker thiophene donor group. The decrease in oxidation potential is consistent with the electrochemical behavior of **iI-T** and **iI-3T** observed by others.[13,17] The behavior of the polymers at a negative potential is much more dependent on the identity of the acceptor unit. Both of the DA polymers exhibit a single reduction peak; for **iI-T**, this peak is sharp and quasi-reversible, while in **iI-3T**, it is much broader and irreversible. The DAA polymers have more complex reduction behavior; **di-iI-T** exhibits one quasi-reversible reduction, followed by two irreversible reductions at lower potentials, while **di-iI-3T** can be quasi-reversibly reduced twice. Both **bis-iI** polymers show two peaks at negative potentials; however, only in **bis-iI-3T** were both reductions quasi-reversible.

The polymers' HOMO and LUMO energies were estimated from the onset of oxidation and reduction using differential pulse voltammetry, respectively (Figure 3),[15,17,22,23,41] and the electrochemical band gaps ($E_{g,elec}$) are summarized in Table 1. The HOMO levels are largely determined by the identity of the donor unit; in general, the terthiophene-containing polymers have HOMO levels approximately 0.2 eV higher in energy than those of the thiophene-containing polymers. The

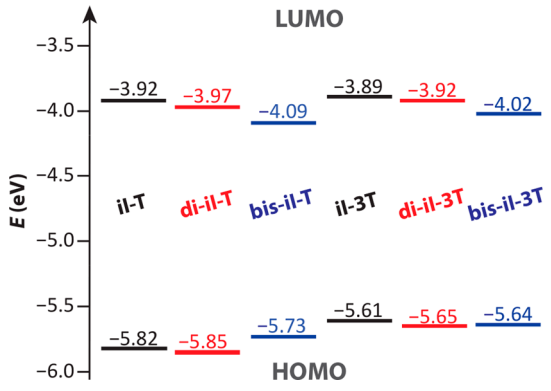

Figure 3. HOMO and LUMO energies of polymers vs vacuum, as estimated from the onset of oxidation and reduction in differential pulse voltammetry; Fc/Fc^+ is assumed to be −5.1 eV vs vacuum.

LUMO energy is much more dependent on the identity of the acceptor unit. The LUMO energies of the **di-iI** polymers are slightly lower than those of the **iI** polymers because of the electron-withdrawing influence of the additional acceptor unit. The decrease in LUMO energy upon addition of a second acceptor is 0.05 eV for the thiophene copolymers (**iI-T** to **di-iI-T**) and 0.03 eV for the terthiophene copolymers (**iI-3T** to **di-iI-3T**). These changes are smaller than those observed in the HOMO when the number of donor units was increased, reflecting the increased torsion between adjacent isoindigo units. Coplanar **bis-iI** is the strongest acceptor unit of those studied; it lowers the LUMO energies of **bis-iI-T** and **bis-iI-3T** by 0.17 and 0.13 eV, respectively, relative to those of their **iI** analogues. These low LUMO levels contribute to the low $E_{g,opt}$ of the **bis-iI** polymers, an important criterion in designing NIR absorbers for OPV applications.

To test the effect of the additional acceptor units on the charge carrier mobilities of our DAA semiconductors, the polymers were used to fabricate bottom-gate bottom-contact OTFTs. Figure 4 compares the average charge carrier

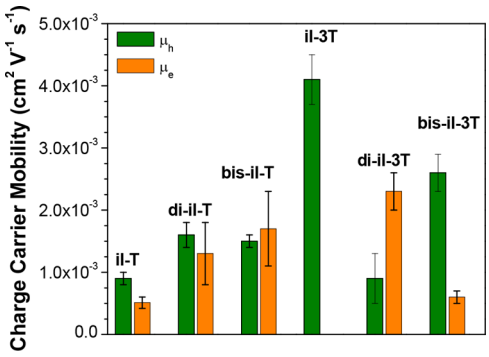

Figure 4. Average charge carrier mobilities of the polymers as measured using bottom-gate bottom-contact OTFTs. Error bars denote plus or minus one standard deviation from the mean, calculated using five devices.

mobilities of the six polymers; representative output and transfer curves of OTFTs made using **di-iI-3T** are shown in Figure 5, with the remainder shown in Figures S10−S14. With the exception of **iI-3T** (which is already known to be a p-type semiconductor),[15] all of the polymers displayed ambipolar charge transport behavior (Table 1). In all cases, the DAA polymers had electron mobilities that were higher than those of their DA analogues. This demonstrates the ability to systematically tune the electron mobilities of DA polymers by inserting additional acceptor units into the polymer repeat unit; however, it is impossible to completely ascribe these changes to electronic effects, as changes in molecular packing may also play a role. In addition to better electron transport, both **di-iI-T** and **bis-iI-T** also had hole mobilities slightly higher than that of **iI-T**; this improvement may be due to changes in the polymer packing induced by the presence of the extended isoindigo units. Of all six polymers, **iI-3T** showed the highest hole mobility [$(4.1 \pm 0.4) \times 10^{-3}$ cm^2 V^{-1} s^{-1}]; this is unsurprising, given that it has the highest donor/acceptor ratio and also the highest HOMO energy of all six polymers. The charge carrier mobility of **bis-iI-T** is similar to that reported by Jiang et al. ($\mu_h = 3.0 \times 10^{-3}$ cm^2 V^{-1} s^{-1}, and $\mu_e = 3.7 \times 10^{-3}$ cm^2 V^{-1} s^{-1});[39] the small difference is likely due to different interchain packing, resulting from the different alkyl sub-

DOI: 10.1021/acs.chemmater.8b02535
Chem. Mater. 2018, 30, 4864−4873

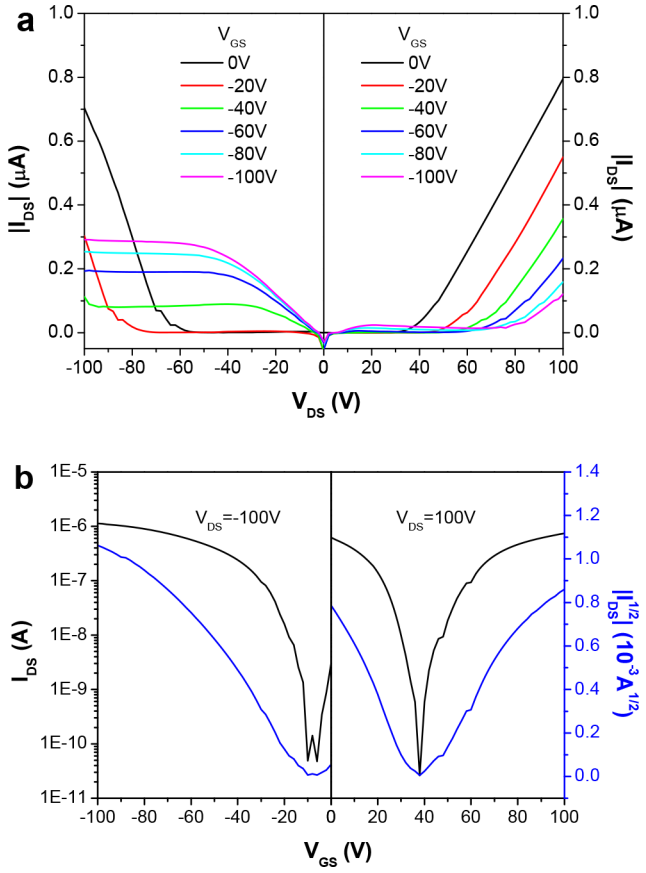

Figure 5. (a) Output and (b) transfer curves of bottom-gate bottom-contact OTFTs made using **di-iI-3T**, annealed at 50 °C.

stituents used.[42−44] The polymer with the highest electron mobility [(2.3 ± 0.3) × 10^{-3} cm^2 V^{-1} s^{-1}] was **di-iI-3T**, again highlighting the impact of adding additional electron acceptors to the polymer repeat unit.

Having established that all six polymers are capable of p-type transport, we evaluated their performance as the p-type material in OPVs. The polymers were tested in a bulk heterojunction active layer alongside $PC_{71}BM$, using an ITO/ZnO/polymer:$PC_{71}BM$/MoO_{3-x}/Ag device architecture. The results are summarized in Table 2, and the current−voltage (J−V) curves of the champion devices for each polymer are shown in Figure 6. Both **iI-T** and **iI-3T** have been tested in OPVs by others and are well-studied.[13−17,22,23] The performance of our **iI-T**:$PC_{71}BM$ OPVs is consistent with published results;[17] however, the average PCE of the **iI-3T**:$PC_{71}BM$-based devices reported here (4.2 ± 0.3%) is slightly lower than that reported by others (6.5 ± 0.2%).[17] This is likely due to the lower molecular weight of the **iI-3T** used in this work (M_n = 27 kDa); previous studies by Ma et al. found an improvement in the maximum PCE of **iI-3T**-based OPVs (from 6.3 to 6.9%) when M_n improved from 43 to 100 kDa.[13] This molecular weight dependence is likely amplified in the lower-M_n sample studied here. Comparing the device performance of all six polymers, we can identify several distinct trends. The open-circuit voltage (V_{oc}) and fill factor (FF) are similar for all polymers with the same donor unit. Because the V_{oc} is primarily governed by the energy difference between the HOMO of the donor polymer and the LUMO of the fullerene (and the HOMO energy is primarily set by the number of thiophene units in the donor), the V_{oc} decreases when the donor changes from thiophene to terthiophene. This is somewhat offset by an increase in the device fill factor with the terthiophene donors. However, the largest difference in performance between the various polymers is a decrease in short-circuit current density (J_{sc}) as the acceptor is changed from **iI** to **di-iI** and **bis-iI**. Both **di-iI-T** and **di-iI-3T** had PCEs lower than those of their isoindigo analogues, owing chiefly to a lower J_{sc}; the **bis-iI** polymers had the lowest PCEs because of low photocurrents.

Because none of the polymers have issues with efficient light absorption (Figure 1), the low photocurrents in the **di-iI**- and **bis-iI**-based polymers must be due to either geminate or bimolecular recombination. The former would be due to inefficient exciton dissociation, while low carrier mobility or trap state formation may lead to the latter. The OTFT data (Figure 4) show that there is only a small difference between the hole mobilites of **di-iI-3T** and **bis-iI-3T** as compared to that of **iI-3T**, while the hole mobilities of **di-iI-T** and **bis-iI-T** were even slightly higher than the hole mobility of **iI-T**. Although charge carrier mobilites derived from OTFT measurements reflect charge transport in the horizontal plane, rather than in the vertical direction (as in the OPV devices), we believe that the small differences in carrier mobility are unlikely to account for the pronounced differences in J_{sc}. Assuming that the trap state density does not depend on the polymer identity, then it is more likely that geminate recombination processes are responsible for the low J_{sc} observed in the **di-iI** and **bis-iI** systems.

The other explanation for the low J_{sc} is that inefficient exciton dissociation in the OPV active layer leads to substantial geminate recombination and a lack of free charge carriers. This could be caused by phase domains that are overly large (preventing excitons from reaching a donor−acceptor junction) or by slow rates of electron transfer at the interface. The exciton diffusion length in organic semiconductors is typically ∼10 nm; therefore, phase domains must be comparably sized for efficient exciton separation.[45] Atomic

Table 2. Device Performance Parameters for OPVs with an ITO/ZnO/Polymer:$PC_{71}BM$/MoO_x/Ag Architecture[a]

polymer	V_{oc} (V)	J_{sc} (mA cm^{-2})	fill factor (%)	PCE (%)	J_{sc}[b] (mA cm^{-2})
iI-T	0.85 ± 0.02 (0.87)	6.3 ± 0.2 (6.51)	58 ± 1 (58)	3.1 ± 0.1 (3.28)	6.10
iI-3T	0.72 ± 0.01 (0.72)	8.7 ± 0.5 (9.78)	66.8 ± 0.6 (67)	4.2 ± 0.3 (4.73)	9.47
di-iI-T	0.86 ± 0.03 (0.91)	4.2 ± 0.1 (4.55)	50 ± 3 (51)	1.8 ± 0.2 (2.12)	4.68
di-iI-3T	0.77 ± 0.01 (0.79)	5.9 ± 0.3 (6.54)	61 ± 2 (58)	2.8 ± 0.1 (3.04)	6.58
bis-iI-T	0.8 ± 0.1 (0.78)	0.8 ± 0.1 (0.89)	54 ± 8 (59)	0.3 ± 0.1 (0.42)	0.82
bis-iI-3T	0.66 ± 0.01 (0.66)	2.4 ± 0.2 (2.61)	58 ± 4 (62)	0.9 ± 0.1 (1.07)	2.29

[a]Numbers in parentheses are for champion devices. Averages calculated using a minimum of 17 devices. [b]J_{sc} calculated from the IPCE spectrum of the champion cell.

DOI: 10.1021/acs.chemmater.8b02535
Chem. Mater. 2018, 30, 4864−4873

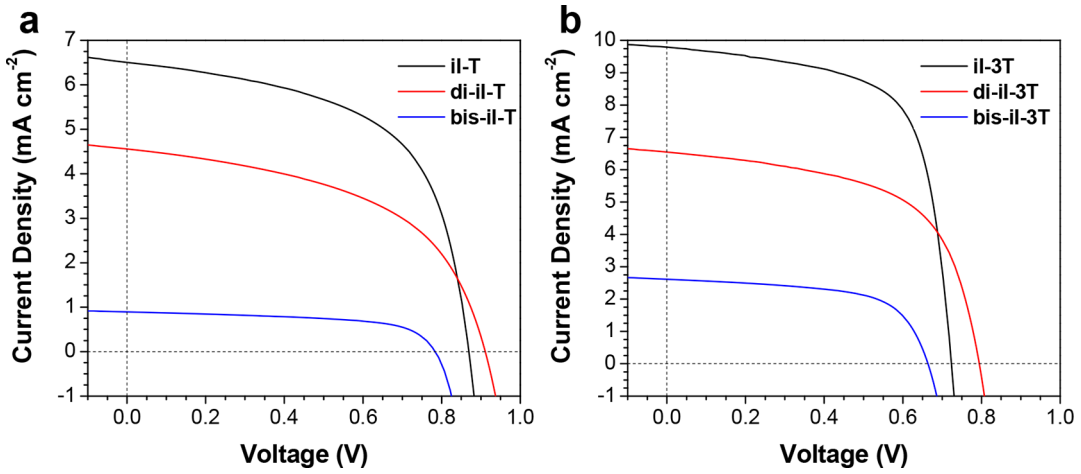

Figure 6. $J-V$ curves of champion OPVs with an ITO/ZnO/polymer:$PC_{71}BM$/MoO_x/Ag architecture: (a) **iI-T**, **di-iI-T**, and **bis-iI-T** and (b) **iI-3T**, **di-iI-3T**, and **bis-iI-3T**.

force microscopy (AFM) and GIWAXS were therefore used to assess the morphology and crystallinity of the OPV active layers. AFM height images (1 μm × 1 μm) of the active layers were recorded (Figure 7), and the root-mean-square roughness

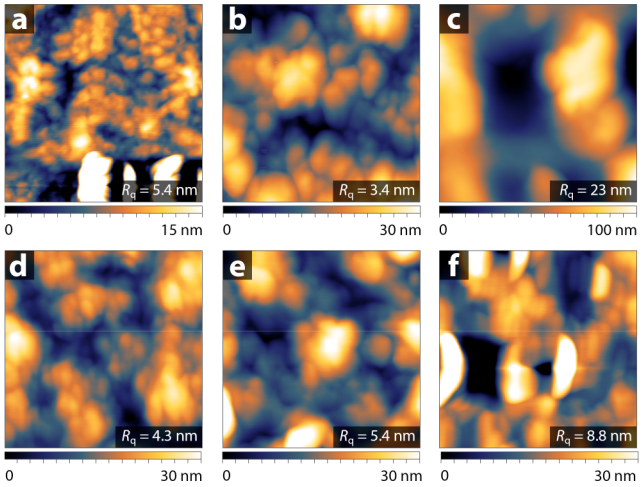

Figure 7. AFM height images (1 μm × 1 μm) of polymer:$PC_{71}BM$ OPV active layer blends: (a) **iI-T**, (b) **di-iI-T**, (c) **bis-iI-T**, (d) **iI-3T**, (e) **di-iI-3T**, and (f) **bis-iI-3T**.

(R_q) was calculated. The AFM images of the **iI-T**:$PC_{71}BM$ and **iI-3T**:$PC_{71}BM$ active layers were similar to those reported by others,[17] and the morphologies of the **di-iI**-based active layers were very similar to those of the **iI**-based analogues (R_q = 3−5 nm). In contrast, the **bis-iI-T** and **bis-iI-3T** phase domains were coarser, with root-mean-square roughnesses of 23 and 9 nm, respectively. However, while both **bis-iI-T** and **bis-iI-3T** displayed approximately the same drop in photovoltaic performance relative to the **di-iI** and **iI** polymers, the **bis-iI-T** domains were noticeably coarser than those in the **bis-iI-3T** system. This lack of correlation between the film morphology and the device performance makes it unlikely that a change in the active layer morphology is the sole cause of the drop in OPV efficiency, although it may play a contributing role.

The crystallinity of the polymers in pristine thin films as well as in blends with $PC_{71}BM$ was evaluated by GIWAXS (Figure 8 and Figures S15 and S16). GIWAXS patterns of **iI-T** and **iI-3T** have previously been reported by Grand et al.;[17] the principal peaks at 0.3 and 1.6 Å^{-1} were assigned to the (100) and (010) reflections, respectively.[15,17] The (100) and (010) planes represent the interchain lamellar packing and π-stacking interactions, respectively. The GIWAXS patterns of all six polymers in this study were found to be similar to those previously reported for **iI-T** and **iI-3T**. With the exception of **iI-3T**, the polymers show preferential face-on orientation to the substrate in the as-cast (Figure S15) and annealed (Figure S16) films, as evidenced by the greater intensity of the (010) peak along the q_z axis and the (100) peak along the q_r axis. Conversely, **iI-3T** appears to exhibit a preferential edge-on orientation, with a (100) maximum along the q_z axis; the (010) signal along the q_r axis was obscured by shadowing from the sample stage. The d spacing of the (100) and (010) planes has been reported to be approximately 20−22 Å for the lamellar packing (100) and 3.7−3.8 Å for the π-stacking (010) in **iI-T** and **iI-3T**;[17] this is similar to the d spacing distance found for **di-iI-3T** and **bis-iI-3T** (Table S1). However, **di-iI-T** and **bis-iI-T** both had a π-stacking distance of 4.0 Å, 0.2 Å longer than that in **iI-T**. The increased $\pi-\pi$ distance for **di-iI-T** and **bis-iI-**

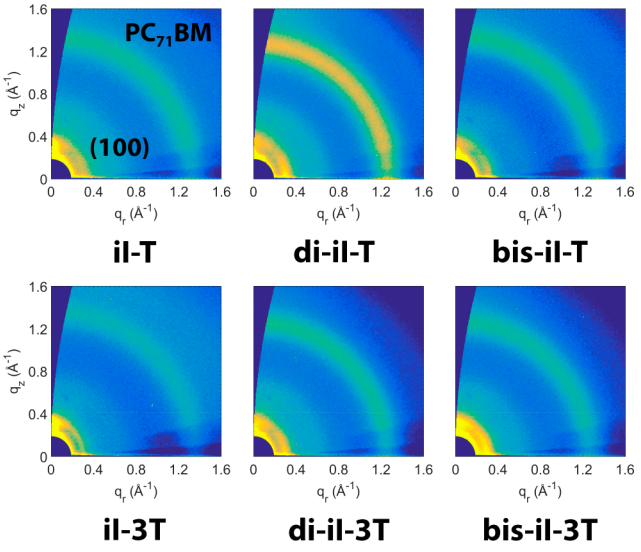

Figure 8. GIWAXS patterns of as-cast polymer:$PC_{71}BM$ active layer blends.

DOI: 10.1021/acs.chemmater.8b02535
Chem. Mater. 2018, 30, 4864−4873

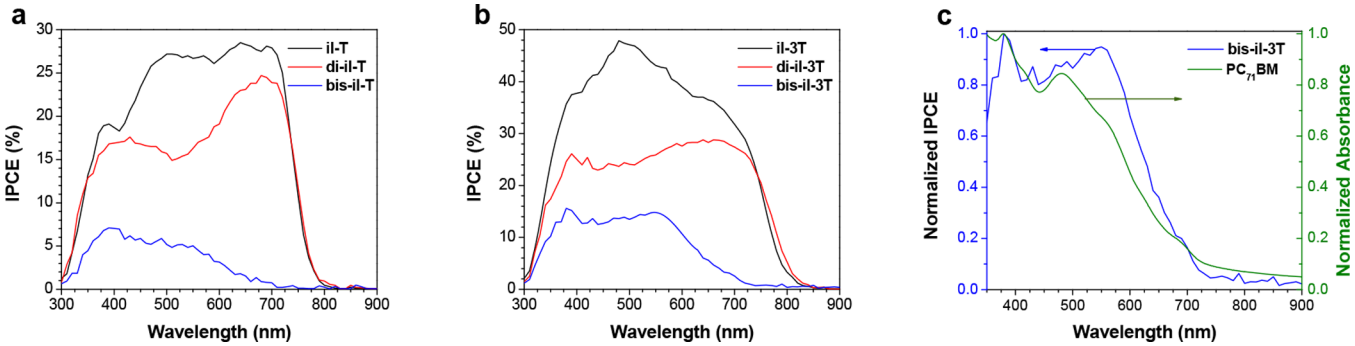

Figure 9. IPCE spectra of champion polymer:$PC_{71}BM$ OPVs: (a) **iI-T**, **di-iI-T**, and **bis-iI-T** and (b) **iI-3T**, **di-iI-3T**, and **bis-iI-3T**. (c) Normalized IPCE spectrum of the champion **bis-iI-3T**:$PC_{71}BM$ device and the normalized thin film absorbance spectrum of $PC_{71}BM$.

T may be due to the difference in the relative size of the donor and acceptor units. The GIWAXS patterns of the OPV active layer blends are shown in Figure 8; in addition to the (100) reflection for each polymer, an isotropic peak attributed to $PC_{71}BM$ is seen at ∼1.3 $Å^{-1}$.[46] The similarity of the patterns for all six blends suggests that there are no drastic differences in the crystallinity of the films that can solely account for the variation in OPV performance.

Given the similarity of the morphology and crystallinity for all six polymers, they are unlikely to be the only factors responsible for the observed trends in OPV performance. Another possible cause of the lower photocurrents in the **di-iI** and **bis-iI** polymers is a low energetic driving force for exciton dissociation. Because excitons in organic semiconductors are relatively tightly bound, an energetic driving force must be present to promote electron transfer from the LUMO of the p-type semiconductor to that of the n-type semiconductor. From Figure 3, it is obvious that the polymer LUMO energies are controlled by the acceptor and decrease in the following order: **iI** > **di-iI** > **bis-iI**; the decrease in LUMO energy correlates very well with the drop in J_{sc}. The LUMO level of $PC_{71}BM$ is reported to lie between −4.0 and −4.2 eV versus vacuum,[12,47] and a minimum LUMO−LUMO offset in the range of 0.1−0.5 eV is typically required to drive electron transfer.[1,2,48,49] Because the LUMO levels of **bis-iI-T** and **bis-iI-3T** are slightly below −4.0 eV versus vacuum (Figure 3), inefficient exciton dissociation is certainly a possible cause of the trends in J_{sc}.

The incident photon to current efficiency (IPCE) spectra (Figure 9) support this hypothesis, especially for **bis-iI-T** and **bis-iI-3T**. The IPCE spectra of OPVs based on the **iI** and **di-iI** polymers closely match the UV−vis spectra of the polymer films (Figure 1), and the onset of photocurrent production is at the $E_{g,opt}$ of the polymer. The IPCE spectra of OPVs made using **bis-iI-T** and **bis-iI-3T** are distinctly different; despite the fact that these polymers absorb well out to 950 nm, negligible photocurrent is produced beyond 700 nm. While these IPCE spectra do not match the UV−vis absorbance spectra of the polymers, Figure 9c overlays the normalized IPCE spectrum of a **bis-iI-3T**:$PC_{71}BM$-based OPV with the normalized thin film absorbance spectrum of $PC_{71}BM$. These spectra match very well, and the onset of photocurrent production is at the HOMO−LUMO gap of the fullerene. This implies that excitons generated in the **bis-iI** polymers are not dissociating and that the majority of photocurrent in these OPVs is generated by fullerene-based excitons. In this case, the driving force for exciton dissociation is governed not by the LUMO−LUMO offset but by the offset of the HOMO levels of the two semiconductors. The HOMO level of $PC_{71}BM$ is approximately −6.10 eV versus vacuum;[12] there is a substantial enough HOMO−HOMO offset with **bis-iI-3T** (−5.64 eV vs vacuum) to provide the energetic driving force for exciton dissociation. The IPCE spectra combined with the measurements of the LUMO level demonstrate that as the acceptor strength of the polymers is increased, the energetic driving force for exciton dissociation decreases. As this process becomes less energetically favorable, the J_{sc} decreases. In the extreme case of the **bis-iI** polymers, there is no longer sufficient driving force for electron transfer between the p- and n-type semiconductors, and the efficiency of the OPV decreases dramatically.

■ CONCLUSION

To study the impact of acceptor length and planarity on the optoelectronic properties of donor−acceptor systems, we synthesized a series of four DAA copolymers based on thiophene donors and isoindigo-based acceptors. The optoelectronic properties of these four DAA copolymers were compared to those of the analogous, well-studied, DA copolymers. We found that increasing the number of acceptors in the polymer repeat unit decreased the LUMO energy of the polymer and increased the electron mobility; this effect was amplified when the two acceptor units were fused together in a coplanar fashion. These changes can have a pronounced effect on the performance of optoelectronic devices, as illustrated here with both OTFTs and OPVs. We believe that changing the number of acceptors in the polymer repeat unit is a general strategy that could be used to fine-tune the properties of donor−acceptor systems, leading to better materials with precisely tailored frontier orbital energies and charge carrier mobilities.

■ ASSOCIATED CONTENT

Supporting Information

The Supporting Information is available free of charge on the ACS Publications website at DOI: 10.1021/acs.chemmater.8b02535.

Materials and characterization methods, detailed synthetic procedures, cyclic and differential pulse voltammograms, thin film GIWAXS patterns, and OTFT output and transfer curves (PDF)

■ AUTHOR INFORMATION

Corresponding Author

*E-mail: tim.kelly@usask.ca. Fax: +1-306-966-4730. Telephone: +1-306-966-4666.

DOI: 10.1021/acs.chemmater.8b02535
Chem. Mater. 2018, 30, 4864−4873

ORCID
Nicholas M. Randell: 0000-0001-9408-3510
Yuning Li: 0000-0003-3679-8133
Timothy L. Kelly: 0000-0002-2907-093X

Notes
The authors declare no competing financial interest.

■ ACKNOWLEDGMENTS

The Natural Science and Engineering Research Council of Canada (NSERC, RGPIN-2017-03732) and the University of Saskatchewan are acknowledged for financial support. T.L.K. is a Canada Research Chair in Photovoltaics. This research was undertaken in part, thanks to funding from the Canada Research Chairs Program. N.M.R. and C.L.R. thank the NSERC for scholarship funding. The GIWAXS experiments described in this paper were performed at the Canadian Light Source, which is supported by the Canada Foundation for Innovation, NSERC, the University of Saskatchewan, the Government of Saskatchewan, Western Economic Diversification Canada, the National Research Council Canada, and the Canadian Institutes of Health Research. Technical support from HXMA beamline scientist Dr. Chang-Yong Kim is gratefully acknowledged. Federico Cruciani and Prof. Pierre Beaujuge (KAUST) are gratefully acknowledged for the SEC analysis.

■ REFERENCES

(1) Brabec, C. J.; Gowrisanker, S.; Halls, J. J. M.; Laird, D.; Jia, S.; Williams, S. P. Polymer-Fullerene Bulk-Heterojunction Solar Cells. *Adv. Mater.* **2010**, *22*, 3839−3856.
(2) Scharber, M. C.; Mühlbacher, D.; Koppe, M.; Denk, P.; Waldauf, C.; Heeger, A. J.; Brabec, C. J. Design Rules for Donors in Bulk-Heterojunction Solar Cells—Towards 10% Energy-Conversion Efficiency. *Adv. Mater.* **2006**, *18*, 789−794.
(3) Heeger, A. J. Semiconducting Polymers: the Third Generation. *Chem. Soc. Rev.* **2010**, *39*, 2354−2371.
(4) Zhang, Q. T.; Tour, J. M. Alternating Donor/Acceptor Repeat Units in Polythiophenes. Intramolecular Charge Transfer for Reducing Band Gaps in Fully Substituted Conjugated Polymers. *J. Am. Chem. Soc.* **1998**, *120*, 5355−5362.
(5) Dou, L.; Liu, Y.; Hong, Z.; Li, G.; Yang, Y. Low-Bandgap Near-IR Conjugated Polymers/Molecules for Organic Electronics. *Chem. Rev.* **2015**, *115*, 12633−12665.
(6) Blouin, N.; Michaud, A.; Leclerc, M. A Low-Bandgap Poly(2,7-Carbazole) Derivative for Use in High-Performance Solar Cells. *Adv. Mater.* **2007**, *19*, 2295−2300.
(7) Blouin, N.; Michaud, A.; Gendron, D.; Wakim, S.; Blair, E.; Neagu-Plesu, R.; Belletête, M.; Durocher, G.; Tao, Y.; Leclerc, M. Toward a Rational Design of Poly(2,7-Carbazole) Derivatives for Solar Cells. *J. Am. Chem. Soc.* **2008**, *130*, 732−742.
(8) Qu, S.; Tian, H. Diketopyrrolopyrrole (DPP)-Based Materials for Organic Photovoltaics. *Chem. Commun.* **2012**, *48*, 3039−3051.
(9) Zheng, Y.-Q.; Wang, Z.; Dou, J.-H.; Zhang, S.-D.; Luo, X.-Y.; Yao, Z.-F.; Wang, J.-Y.; Pei, J. Effect of Halogenation in Isoindigo-Based Polymers on the Phase Separation and Molecular Orientation of Bulk Heterojunction Solar Cells. *Macromolecules* **2015**, *48*, 5570−5577.
(10) Lei, T.; Dou, J.-H.; Ma, Z.-J.; Liu, C.-J.; Wang, J.-Y.; Pei, J. Chlorination as a Useful Method to Modulate Conjugated Polymers: Balanced and Ambient-Stable Ambipolar High-Performance Field-Effect Transistors and Inverters Based on Chlorinated Isoindigo Polymers. *Chem. Sci.* **2013**, *4*, 2447−2452.
(11) Lei, T.; Dou, J.-H.; Ma, Z.-J.; Yao, C.-H.; Liu, C.-J.; Wang, J.-Y.; Pei, J. Ambipolar Polymer Field-Effect Transistors Based on Fluorinated Isoindigo: High Performance and Improved Ambient Stability. *J. Am. Chem. Soc.* **2012**, *134*, 20025−20028.
(12) Zhou, N.; Guo, X.; Ortiz, R. P.; Harschneck, T.; Manley, E. F.; Lou, S. J.; Hartnett, P. E.; Yu, X.; Horwitz, N. E.; Burrezo, P. M.; Aldrich, T. J.; López Navarrete, J. T.; Wasielewski, M. R.; Chen, L. X.; Chang, R. P. H.; Facchetti, A.; Marks, T. J. Marked Consequences of Systematic Oligothiophene Catenation in Thieno[3,4- C]Pyrrole-4,6-Dione and Bithiopheneimide Photovoltaic Copolymers. *J. Am. Chem. Soc.* **2015**, *137*, 12565−12579.
(13) Ma, Z.; Sun, W.; Himmelberger, S.; Vandewal, K.; Tang, Z.; Bergqvist, J.; Salleo, A.; Andreasen, J. W.; Inganäs, O.; Andersson, M. R.; Muller, C.; Zhang, F.; Wang, E. Structure−Property Relationships of Oligothiophene−Isoindigo Polymers for Efficient Bulk-Heterojunction Solar Cells. *Energy Environ. Sci.* **2014**, *7*, 361−369.
(14) Ho, C.-C.; Chen, C.-A.; Chang, C.-Y.; Darling, S. B.; Su, W.-F. Isoindigo-Based Copolymers for Polymer Solar Cells with Efficiency Over 7%. *J. Mater. Chem. A* **2014**, *2*, 8026−8032.
(15) Stalder, R.; Puniredd, S. R.; Hansen, M. R.; Koldemir, U.; Grand, C.; Zajaczkowski, W.; Müllen, K.; Pisula, W.; Reynolds, J. R. Ambipolar Charge Transport in Isoindigo-Based Donor−Acceptor Polymers. *Chem. Mater.* **2016**, *28*, 1286−1297.
(16) Lai, T.-H.; Constantinou, I.; Grand, C. M.; Klump, E. D.; Baek, S.; Hsu, H.-Y.; Tsang, S.-W.; Schanze, K. S.; Reynolds, J. R.; So, F. Evidence of Molecular Structure Dependent Charge Transfer Between Isoindigo-Based Polymers and Fullerene. *Chem. Mater.* **2016**, *28*, 2433−2440.
(17) Grand, C.; Baek, S.; Lai, T.-H.; Deb, N.; Zajaczkowski, W.; Stalder, R.; Müllen, K.; Pisula, W.; Bucknall, D. G.; So, F.; Reynolds, J. R. Structure−Property Relationships Directing Transport and Charge Separation in Isoindigo Polymers. *Macromolecules* **2016**, *49*, 4008−4022.
(18) Mei, J.; Graham, K. R.; Stalder, R.; Reynolds, J. R. Synthesis of Isoindigo-Based Oligothiophenes for Molecular Bulk Heterojunction Solar Cells. *Org. Lett.* **2010**, *12*, 660−663.
(19) Stalder, R.; Mei, J.; Graham, K. R.; Estrada, L. A.; Reynolds, J. R. Isoindigo, a Versatile Electron-Deficient Unit for High-Performance Organic Electronics. *Chem. Mater.* **2014**, *26*, 664−678.
(20) Wang, E.; Mammo, W.; Andersson, M. R. 25th Anniversary Article: Isoindigo-Based Polymers and Small Molecules for Bulk Heterojunction Solar Cells and Field Effect Transistors. *Adv. Mater.* **2014**, *26*, 1801−1826.
(21) Stalder, R.; Mei, J.; Reynolds, J. R. Isoindigo-Based Donor−Acceptor Conjugated Polymers. *Macromolecules* **2010**, *43*, 8348−8352.
(22) Wang, E.; Ma, Z.; Zhang, Z.; Vandewal, K.; Henriksson, P.; Inganäs, O.; Zhang, F.; Andersson, M. R. An Easily Accessible Isoindigo-Based Polymer for High-Performance Polymer Solar Cells. *J. Am. Chem. Soc.* **2011**, *133*, 14244−14247.
(23) Wang, E.; Ma, Z.; Zhang, Z.; Henriksson, P.; Inganäs, O.; Zhang, F.; Andersson, M. R. An Isoindigo-Based Low Band Gap Polymer for Efficient Polymer Solar Cells with High Photo-Voltage. *Chem. Commun.* **2011**, *47*, 4908−4910.
(24) Deng, P.; Zhang, Q. Recent Developments on Isoindigo-Based Conjugated Polymers. *Polym. Chem.* **2014**, *5*, 3298−3305.
(25) Stalder, R.; Mei, J.; Subbiah, J.; Grand, C.; Estrada, L. A.; So, F.; Reynolds, J. R. N-Type Conjugated Polyisoindigos. *Macromolecules* **2011**, *44*, 6303−6310.
(26) Grenier, F.; Aïch, B. R.; Lai, Y.-Y.; Guérette, M.; Holmes, A. B.; Tao, Y.; Wong, W. W. H.; Leclerc, M. Electroactive and Photoactive Poly[Isoindigo -Alt-EDOT] Synthesized Using Direct (Hetero)-Arylation Polymerization in Batch and in Continuous Flow. *Chem. Mater.* **2015**, *27*, 2137−2143.
(27) Grenier, F.; Berrouard, P.; Pouliot, J.-R.; Tseng, H.-R.; Heeger, A. J.; Leclerc, M. Synthesis of New N-Type Isoindigo Copolymers. *Polym. Chem.* **2013**, *4*, 1836−1841.
(28) Ashraf, R. S.; Kronemeijer, A. J.; James, D. I.; Sirringhaus, H.; McCulloch, I. A New Thiophene Substituted Isoindigo Based Copolymer for High Performance Ambipolar Transistors. *Chem. Commun.* **2012**, *48*, 3939−3941.
(29) Koizumi, Y.; Ide, M.; Saeki, A.; Vijayakumar, C.; Balan, B.; Kawamoto, M.; Seki, S. Thienoisoindigo-Based Low-Band Gap

DOI: 10.1021/acs.chemmater.8b02535
Chem. Mater. 2018, 30, 4864−4873

Polymers for Organic Electronic Devices. *Polym. Chem.* **2013**, *4*, 484−494.
(30) Li, S.; Yuan, Z.; Yuan, J.; Deng, P.; Zhang, Q.; Sun, B. An Expanded Isoindigo Unit as a New Building Block for a Conjugated Polymer Leading to High-Performance Solar Cells. *J. Mater. Chem. A* **2014**, *2*, 5427−5433.
(31) Lei, T.; Dou, J.-H.; Cao, X.-Y.; Wang, J.-Y.; Pei, J. A BDOPV-Based Donor-Acceptor Polymer for High-Performance N-Type and Oxygen-Doped Ambipolar Field-Effect Transistors. *Adv. Mater.* **2013**, *25*, 6589−6593.
(32) Dou, J.-H.; Zheng, Y.-Q.; Yao, Z.-F.; Yu, Z.-A.; Lei, T.; Shen, X.; Luo, X.-Y.; Sun, J.; Zhang, S.-D.; Ding, Y.-F.; Han, G.; Yi, Y.; Wang, J.-Y.; Pei, J. Fine-Tuning of Crystal Packing and Charge Transport Properties of BDOPV Derivatives Through Fluorine Substitution. *J. Am. Chem. Soc.* **2015**, *137*, 15947−15956.
(33) Lei, T.; Dou, J.-H.; Cao, X.-Y.; Wang, J.-Y.; Pei, J. Electron-Deficient Poly(P-Phenylene Vinylene) Provides Electron Mobility Over 1 $cm^2 \cdot V^{-1} s^{-1}$ under Ambient Conditions. *J. Am. Chem. Soc.* **2013**, *135*, 12168−12171.
(34) Cao, Y.; Yuan, J.-S.; Zhou, X.; Wang, X.-Y.; Zhuang, F.-D.; Wang, J.-Y.; Pei, J. N-Fused BDOPV: a Tetralactam Derivative as a Building Block for Polymer Field-Effect Transistors. *Chem. Commun.* **2015**, *51*, 10514−10516.
(35) He, Y.; Guo, C.; Sun, B.; Quinn, J.; Li, Y. (3E,7E)-3,7-Bis(2-Oxoindolin-3-Ylidene)-5,7- Dihydropyrrolo[2,3-f]Indole-2,6-(1H,3H)-Dione Based Polymers for Ambipolar Organic Thin Film Transistors. *Chem. Commun.* **2015**, *51*, 8093−8096.
(36) Chen, M. S.; Niskala, J. R.; Unruh, D. A.; Chu, C. K.; Lee, O. P.; Fréchet, J. M. J. Control of Polymer-Packing Orientation in Thin Films Through Synthetic Tailoring of Backbone Coplanarity. *Chem. Mater.* **2013**, *25*, 4088−4096.
(37) James, D. I.; Wang, S.; Ma, W.; Hedström, S.; Meng, X.; Persson, P.; Fabiano, S.; Crispin, X.; Andersson, M. R.; Berggren, M.; Wang, E. High-Performance Hole Transport and Quasi-Balanced Ambipolar OFETs Based on D-A-A Thieno-Benzo-Isoindigo Polymers. *Adv. Electron. Mater.* **2016**, *2*, 1500313.
(38) Randell, N. M.; Boutin, P. C.; Kelly, T. L. Bisisoindigo: Using a Ring-Fusion Approach to Extend the Conjugation Length of Isoindigo. *J. Mater. Chem. A* **2016**, *4*, 6940−6945.
(39) Jiang, Y.; Gao, Y.; Tian, H.; Ding, J.; Yan, D.; Geng, Y.; Wang, F. Synthesis and Characterization of Isoindigo[7,6-g]Isoindigo-Based Donor−Acceptor Conjugated Polymers. *Macromolecules* **2016**, *49*, 2135−2144.
(40) Xu, L.; Zhao, Z.; Xiao, M.; Yang, J.; Xiao, J.; Yi, Z.; Wang, S.; Liu, Y. π-Extended Isoindigo-Based Derivative: a Promising Electron-Deficient Building Block for Polymer Semiconductors. *ACS Appl. Mater. Interfaces* **2017**, *9*, 40549−40555.
(41) Cardona, C. M.; Li, W.; Kaifer, A. E.; Stockdale, D.; Bazan, G. C. Electrochemical Considerations for Determining Absolute Frontier Orbital Energy Levels of Conjugated Polymers for Solar Cell Applications. *Adv. Mater.* **2011**, *23*, 2367−2371.
(42) Mei, J.; Bao, Z. Side Chain Engineering in Solution-Processable Conjugated Polymers. *Chem. Mater.* **2014**, *26*, 604−615.
(43) Li, Y.; Feng, Q.; Ling, H.; Chang, Y.; Liu, Z.; Liu, H.; Xie, L.; Yin, C.; Yi, M.; Huang, W. Bulky Side Chain Effect of Poly(N-Vinylcarbazole)-Based Stacked Polymer Electrets on Device Performance Parameters of Transistor Memories. *J. Polym. Sci., Part A: Polym. Chem.* **2017**, *55*, 3554−3564.
(44) Kang, B.; Kim, R.; Lee, S. B.; Kwon, S.-K.; Kim, Y.-H.; Cho, K. Side-Chain-Induced Rigid Backbone Organization of Polymer Semiconductors Through Semifluoroalkyl Side Chains. *J. Am. Chem. Soc.* **2016**, *138*, 3679−3686.
(45) Mikhnenko, O. V.; Blom, P. W. M.; Nguyen, T.-Q. Exciton Diffusion in Organic Semiconductors. *Energy Environ. Sci.* **2015**, *8*, 1867−1888.
(46) Xiao, T.; Xu, H.; Grancini, G.; Mai, J.; Petrozza, A.; Jeng, U.-S.; Wang, Y.; Xin, X.; Lu, Y.; Choon, N. S.; Xiao, H.; Ong, B. S.; Lu, X.; Zhao, N. Molecular Packing and Electronic Processes in Amorphous-Like Polymer Bulk Heterojunction Solar Cells with Fullerene Intercalation. *Sci. Rep.* **2015**, *4*, 5211.
(47) Liao, S.-H.; Jhuo, H.-J.; Cheng, Y.-S.; Chen, S.-A. Fullerene Derivative-Doped Zinc Oxide Nanofilm as the Cathode of Inverted Polymer Solar Cells with Low-Bandgap Polymer (PTB7-Th) for High Performance. *Adv. Mater.* **2013**, *25*, 4766−4771.
(48) Ostroverkhova, O. Organic Optoelectronic Materials: Mechanisms and Applications. *Chem. Rev.* **2016**, *116*, 13279−13412.
(49) Brédas, J.-L.; Beljonne, D.; Coropceanu, V.; Cornil, J. Charge-Transfer and Energy-Transfer Processes in π-Conjugated Oligomers and Polymers: a Molecular Picture. *Chem. Rev.* **2004**, *104*, 4971−5004.

DOI: 10.1021/acs.chemmater.8b02535
Chem. Mater. 2018, 30, 4864−4873